Supporting Information

Solvent-free, non-thermal destruction of PFAS chemicals and PFAS in sediment by piezoelectric ball milling

Nanyang Yang,[1†] Shasha Yang,[1,2†] Qingquan Ma,[3] Claudia Beltran,[1] Yunqiao Guan[1], Madison Morsey,[4] Elizabeth Brown,[1] Sujan Fernando,[1] Thomas Holsen,[1] Wen Zhang,[3] Yang Yang[1*]

[1] Department of Civil and Environmental Engineering, Clarkson University, Potsdam, New York 13699, United States

[2] Institute for a Sustainable Environment, Clarkson University, Potsdam, New York 13699, United States

[3] John A. Reif, Jr. Department of Civil and Environmental Engineering, New Jersey Institute of Technology, Newark, New Jersey 07102, United States

[4] Department of Chemistry and Biomolecular Science, Clarkson University, Potsdam, New York 13699, United States

* Corresponding author: Email: [redacted]@clarkson.edu. Phone: [redacted]

† These authors contributed equally.

Text S1. Chemicals and Ball Mill Operation.

All the reagents used were at least analytical grade, except as noted. Boron nitride (BN), Potassium hydroxide (KOH), formic acid (HCOOH), Supelclean ENVI-Carb, Perfluorooctanoic acid (PFOA), Heptadecafluorooctanesulfonic acid potassium salt (PFOS) were obtained from Sigma-Aldrich Co. (USA). Acetonitrile was purchased from Fisher Scientific. Superclean ENVI-Carb was purchased from SUPELCO, Inc (PA, USA).

Ball milling treatment was conducted on a planetary ball mill (PQ-N04, Across International, USA). The mill has four stainless steel (SS) jars (100 mL) filled with SS balls (10 large balls at a diameter of 10 mm and 106 small balls at a diameter of 6 mm). The SS jars and balls can be replaced with counterparts made of zirconia to exclude the potential interference of iron leaching. PFAS-containing samples (chemicals or sediments) and co-milling reagents were added to the jars, which were then covered by jar lids. All trials were performed at laboratory room temperature and atmospheric pressure. The grinding jar remained closed during milling and was opened for sampling. The atmosphere in the headspace was not deliberately controlled, thereby should be air.

Text S2. Extraction of PFAS from Solid Samples.

For tests aimed to destruct solid PFOA, the solid after ball mill treatment was ultrasonically extracted with 50 mL Milli-Q water for 30 min. After centrifuge separation, the supernatants were diluted by 75%/25% methanol/water and analyzed by UPLC-MS/MS. As for the ball milling destruction of PFOS, the analytical procedure was identical, except methanol was used as the extraction solvent.

The extraction of PFAS from raw and treated sediments follows the procedure described below.

(1) 0.1 g sediment sample was transferred to a polypropylene (PP) centrifuge tube and spiked with 30 µL of isotope-labeled PFAS internal standard (IS) mix (1000 ng/mL each, full list see **Table S1**).

(2) 1.5 mL extraction solvent (acetonitrile with 0.2% formic acid [v/v]) was introduced to the centrifuge tube, followed by 15 min sonication at 60 °C and 5 min centrifugation at 2500 rpm.
(3) The supernatant was transferred to a clean centrifuge tube as the primary extract.
(4) Steps 2 and 3 were repeated once more, resulting in a total extraction volume of 3 mL.
(5) Next, 1 mL aliquot of the extract was transferred to a PP tube to which ~5 mg of Envicarb was added and vortexed for 30 seconds, followed by a 5 min centrifugal separation at 10000 rpm. A 0.1 mL aliquot of this sample was then removed and diluted to 1 mL with 75% Methanol for LC-MS analysis. The concentration of each IS spiked in Step #1 should be diluted to 1 ng/mL correspondingly.
(6) Method blanks were also generated and analyzed following steps #1-5, except no sediment samples were added, and the internal standard mix was added directly in 3 mL extract solvent. The blank test sample was subject to the same sonication extraction, centrifuge separation, and clean-up processes. The IS recovery efficiencies were calculated by comparing the response in the samples and blanks to that of the mid-level calibration standard, which was analyzed alongside. The IS recoveries ranged from 60-110% in this case for all samples analyzed. Details of recovery efficiencies are provided in **Table S1**. The same processing steps include extraction, centrifugation, sonication, cleaning, and dilution for sediment samples extracted after ball milling.

Text S3. LC-MS/MS Analysis

PFAS in extracts were analyzed by ultra-high-performance liquid chromatography (UPLC, Thermo Vanquish) coupled to a triple quadrupole mass spectrometer (MS/MS, Thermo Altis). Briefly, a 5 µL sample was injected and then separated on a Phenomenex Luna Omega column (100 × 2.1 mm, 1.6 µm particle size, C18 stationary phase). The column was maintained at 40 °C at a flow rate was 0.5 mL/min. The mobile phases consisted of 5 mM Ammonium acetate in water (Mobile Phase A) and Acetonitrile (Mobile Phase B). The LC gradient used was as follows: 0 min (30% B), 0.5 min (30% B), 3 min (90% B), 3.1 min (100% B), 4.5 min (100% B), 4.6 min (30% B) and 6.5 min (30%B). Multiple reaction monitoring (MRM) was utilized for MS analysis, whereby the transition

between precursor and fragment ions was monitored. Sample acquisition and analysis were performed with TraceFinder 4.1 (Thermo Scientific).

Text S4. Analysis of Fluoride, Total Fluorine, and Total Organic Fluorine

Fluoride analysis was conducted on a Dionex Integrion ion chromatography system with an anion-exchange column (Thermo Fisher Scientific, RFIC™ IonPac™ AS18 column). AS-18 column was used with a KOH solution (23 mM) as the eluent, flow rate = 1 mL/min, and the suppressor current was set at 57 mA.

Total fluorine (TF) analysis was exclusively adopted in the tests of sediment treatment**.** The combustion ion chromatography (CIC; Metrohm, Switzerland) instrument combines ion chromatography (IC) (930 Compact IC Flex, with conductivity detection), an absorber module where the gaseous compounds of the analytes, formed during combustion, are dissolved and channeled to the IC (920 Absorber Module), and an automatic combustion module (Analytik Jena). The separation of ions occurs on a Metrosep A Supp 5 150/4.0 column combined with a Metrosep A Supp 4/5 guard column. Sediment samples were combusted directly to analyze total fluorine. Other operating conditions used are as follows: 1050 °C combustion temperature, 100 mL/min of argon as the carrier gas; 300 mL/min of oxygen as the combustion gas; Milli-Q (18 mΩ cm; 0.56 µS/cm) water as the absorber solution; 1.0 mL min^{-1} mobile phase (0.32 M/0.10 M sodium carbonate/bicarbonate); 1 mL sample loop; 30 °C column temperature; an eleven-point calibration curve using sodium fluoride (0 to 500 µg/L). All solutions (sample dilutions and standards) were prepared with Milli-Q water. The minimum detection limit (MDL) was 5 µg/L, and the limit of quantification (LOQ) was 20 µg/L.

It is reasonable to assume that TF is a sum of inorganic fluoride (measured by IC) and **total organic fluorine (TOF)**. Therefore, TOF values were calculated by substrating the fluoride amounts (detected in the washing solution by IC, in µmol) from TF (measured by CIC, in µmol).

Text S5. Material Characterization

SEM. Scanning electron microscopy (SEM) images were collected at 2 kV accelerating voltage with beam deceleration to minimize specimen charging. Imaging was collected with a JEOL 7900 FLV FE-SEM.

AFM and PFM analysis. Atomic force microscope (AFM) images were obtained on a Dimension Icon AFM (Bruker, USA). The tapping mode using SCM-PIT-V2 tip (0.1 N/M, Bruker) was used to test the surface topography, and PFM in contact mode was used to investigate the piezoelectric properties in a 15 kHz AC electric field.

The principle of PFM is based on the detection of bias-induced surface deformation. Specifically, it brings a sharp conductive probe into contact with a piezoelectric material. Then, an alternating current (AC) bias is applied to the probe tip to induce the deformation of the sample through a converse piezoelectric effect. The piezoelectric response of the surface is detected as the first harmonic component of bias-induced tip deflection. Height images measured in tapping mode (**Figure S1**) were used as a reference axis for the following testing. **Figure S2** shows the vertical deflection, which ranged from 0.5 to 4 V, of BN particles induced by the bias, and the bright areas indicate the strong indentation regime. As shown in **Figure 1b** of the manuscript, the vertical amplitude signal has a positive linear relationship with the bias voltage. Therefore, the piezoelectric coefficient d_{33} could be quantified by **Eq. S1**

$$d_{33} = A/U = V\delta/U \quad (1)$$

where A is the amplitude (nm), V is the vertical deflection signal of the cantilever (mV, 16 times gain), δ is the calibration constant of the photodetector sensitivity (120.17 nm/V), and U is the amplitude of the testing AC voltage (V). d_{33}, which is the slope of the fitted line of A as a function of U in **Figure 1b**, is given as 19.4 pm/V.

ATR-FTIR. Samples were evaluated using an FTIR spectrometer (Bruker INVENIO R). A Platinum attenuated total reflectance (ATR) accessory with a diamond crystal window was used to collect the FTIR spectra of powder samples. The scan rate is 10 kHz.

XPS. Samples were analyzed using a Surface Science Instruments SSX-100 ESCA Spectrometer with operating pressure ca. $1x10^{-9}$ Torr. Monochromatic Al Kα X rays (1486.6 eV) with photoelectrons collected from an 800 μm diameter sampling area.

Photoelectrons were collected at a 55° emission angle with a source-to-analyzer angle of 70°. A hemispherical analyzer determined electron kinetic energy using a pass energy of 150 eV for wide/survey scans and 50 eV for high-resolution scans. A flood gun was used for charge neutralization of non-conductive samples.

XRD. The XRD patterns (XPERT pro, Malvern Panalytical) were measured using Cu Kα radiation operated at 45 kV, 40 mA at a 2θ angle ranging from 5° to 70° and a scan step size of 0.006°.

Table S1. Summary of recovery efficiencies (RE) and relative standard deviation (RSD) of isotope-labeled PFAS as matrix spike in sediment samples.

Isotope-labeled PFAS standards	**RT (min)**	**RE_1 (%)**	**RE_2 (%)**	**RE_3 (%)**	**RSD (%)**
N-methyl-d_3-perfluoro-1-octanesulfonamidoacetic acid	3.57	73	82	83	7
N-ethyl-d5-perfluoro-1-octanesulfonamidoacetic acid	3.62	86	83	87	2
Sodium 1H,1H,2H,2H-perfluoro (1,2-$^{13}C_2$) hexane sulfonate	1.48	63	67	63	3
Sodium 1H,1H,2H,2H-perfluoro (1,2-$^{13}C_2$) octanesulfonate	2.66	71	63	69	6
Sodium 1H,1H,2H,2H-perfluoro (1,2-$^{13}C_2$) decanesulfonate	2.98	88	89	84	3
Perfllluoro-n(1,2-$^{13}C_2$)-tetradecanoic acid	3.63	92	88	88	3
Potassium perfluoro-1-(2,3,4-$^{13}C_3$) butanesulfonate	1.49	99	101	98	1
Potassium perfluoro-1-(2,3,4-$^{13}C_3$) hexanesulfonate	2.66	101	106	103	2
Perfluoro-n-(1,2,3,4-$^{13}C_4$) heptanoic acid	2.58	118	117	122	2
Perfluoro-n-($^{13}C_5$) pentanoic acid	1	111	109	109	1
Perfluoro-n-(1,2,3,4,6-$^{13}C_5$) hexanoic acid	2.07	109	105	104	2
Perfluoro-n-(1,2,3,4,5,6-$^{13}C_6$) decanoic acid	3.11	92	89	87	3
Perfluoro-n-(1,2,3,4,5,6,7-$^{13}C_7$) undecanoic acid	3.24	92	92	93	1
Perfluoro-1-($^{13}C_8$) octanesulfonamide	3.95	99	98	100	1
Perfluoro-n-($^{13}C_8$) octanoic acid	2.78	102	101	102	1
Sodium perfluoro-1-($^{13}C_8$) octanesulfonate	2.95	74	83	78	6
Perfluoro-n-($^{13}C_9$) nonaoic acid	2.96	84	82	83	2
Perfluoro-n-($^{13}C_4$) butanoic acid	0.51	83	82	82	1
Perfluoro-n-(1,2-$^{13}C_2$) dodecanoic acid	3.38	90	89	90	1

Table S2. Full names, abbreviations, CAS registry numbers, method detection limit (MDL), and mean PFAS concentrations detected in the sediment sample.

No.	Full name	Abbr.	CAS No.	RT (min)[a]	Mean Conc. (μg/g)	Blank (μg/g)	MDL (μg/g)
1	Perfluoro-n-butanoic acid	PFBA	375-22-4	0.77	13.35	ND[b]	0.03
2	Perfluoro-n-pentanoic acid	PFPeA	2706-90-3	0.67	12.83	ND	0.03
3	Perfluoro-n-hexanoic acid	PFHxA	307-24-4	2.07	45.68	ND	0.03
4	Perfluoro-n-heptanoic acid	PFHpA	375-85-9	2.57	8.33	ND	0.03
5	Perfluoro-n-octanoic acid	PFOA	335-67-1	2.78	6.92	ND	0.03
6	Perfluoro-n-nonaoic acid	PFNA	375-95-1	2.96	0.12	ND	0.03
7	Perfluoro-n-decanoic acid	PFDA	335-76-2	3.03	0.07	ND	0.03
8	Perfluoro-n-undecanoic acid	PFUdA	2058-94-8	3.17	ND	ND	0.03
9	Perfluoro-n-dodecanoic acid	PFDoA	307-55-1	3.29	ND	ND	0.03
10	Perflluoro-n-tridecanoic acid	PFTrDA	72629-94-8	3.41	ND	ND	0.03
11	Perflluoro-n-tetradecanoic acid	PFTeDA	376-06-7	3.53	ND	ND	0.03
12	Potassium perfluoro-1-butanesulfonate	PFBS	375-73-5	1.35	12.09	ND	0.03
13	Sodium perfluoro-1-pentanesulfonate	PFPeS	630402-22-1	2.4	10.92	ND	0.03
14	Sodium perfluoro-1-hexanesulfonate	PFHxS: linear	355-46-4	2.63	41.63	ND	0.03
		PFHxS: branched			9.17	ND	0.03
15	Sodium-perfluoro-1-heptanesulfonamide	PFHpS	375-92-8	2.78	4.71	ND	0.03
16	Sodium perfluoro-1-octanesulfonate	PFOS: linear	1763-23-1	2.91	57.36	ND	0.03
		PFOS: branched			53.60	ND	0.03
17	Sodium perfluoro-1-nonanesulfonate	PFNS	98789-57-2	3.02	0.06	ND	0.03
18	Sodium-perfluoro-1-decanesulfonate	PFDS	335-77-3	3.13	0.05	ND	0.03

19	Sodium 1H,1H,2H,2H-perfluorohexane sulfonate	4:2 FTS	757124-72-4	1.26	0.25	ND	0.03
20	Sodium 1H,1H,2H,2H-perfluorooctane sulfonate	6:2FTS	27619-97-2	2.61	3.6	ND	0.03
21	Sodium 1H,1H,2H,2H-perfluorodecane sulfonate	8:2 FTS	39108-34-4	2.92	0.29	ND	0.03
22	Sodium 1H,1H,2H,2H-perfluorododecane sulfonate*	10:2 FTS	N/A	3.18	0.11	ND	0.03
23	Perfluoro-1-octanesulfonamide	FOSA-1	754-91-6	3.87	0.20	ND	0.03
24	Perfluoro-1-octanesulfonamidoacetic acid*	FOSAA	2806-24-8	3.2	ND	ND	0.03
25	N-methylperfluoro-1-octanesulfonamidoacetic acid	N-MeFOSAA	2355-31-9	3.43	ND	ND	0.03
26	N-methylperfluoro-1-octanesulfonamide*	N-MeFOSA-M	31506-32-8	4.36	ND	ND	0.03
27	N-ethylperfluoro-1-octanesulfonamidoacetic acid	N-EtFOSAA	2991-50-6	3.48	ND	ND	0.03
28	N-ethylperfluoro-1-octanesulfonamide*	N-EtFOSA-M	4151-50-2	4.45	ND	ND	0.03
29	Trifluoroacetate	TFA	2923-18-4	0.46	8.15	ND	0.03
30	Perfluoropropanoic acid	PFPA	422-64-0	0.48	8.33	ND	0.03

[a] Retention time in minutes. [b] Not detected.

Table S3. Properties of extract solutions of solid before and after BM treatment

Tests	**BN** [a]		**BN + PFOA** [b]		**Sediment Treatment** [c]			
	Before BM	After BM	Before BM	After BM	Sediment	After BN-BM (6 h)	After BN-BM (10 h)	After KOH-BM (6 h)
pH	8.7	9.8 ± 0.1	2.2 ± 0.1	9.3 ± 0.2	10.4	9.9	-	14.2
Conductivity (mS/cm)	0.02	2.3	2.5 ± 0.5	16.1 ± 0.6	6.1	16.4 ± 0.1	-	84.8 ± 0.7
NH_3-N (mmol) [d]	0.04	2.3 ± 0.5	0.01	9.3 ± 1.2	ND [e]	5.5 ± 0.4	-	-
F^- (µmol)	ND	ND	ND	3409 ± 30	1.7	38.9 ± 0.3	46.3± 6.5	31.5 ± 2.0
TOF (µmol) [f]	-	-	-	-	140	103	96	110

[a] BN powders (19 mmol) were subject to BM treatment for two hours. The treated samples were extracted with 50 mL Milli-Q water. Supernatants were analyzed after centrifuge separation.

[b] PFOA (0.23 mmol) was mixed with BN (19 mmol). Before and after the two-hour BM treatment, mixed solids were extracted with 50 mL DI water. Supernatants were analyzed after centrifuge separation.

[c] Sediment (2 g) was co-milled with 500 mg BN for six hours. Raw and treated sediments were extracted with 40 mL Milli-Q water for analysis. The molar mass of NH_3-N, F^-, and TOF refer to the values measured in the extract solutions.

[d] Ammonia nitrogen (NH_3-N) in the extract solution was measured by HACH method 10031.

[e] Not detected.

[f] Total organic fluorine (TOF) is obtained by subtracting the F^- amount (µmol) from the total fluorine (142 ± 7.6 µmol for 2 g sediment measured by CIC). 2 g sediment contains 140 µmol TOF, giving a value of 70 µmol/g sediments cited in the manuscript.

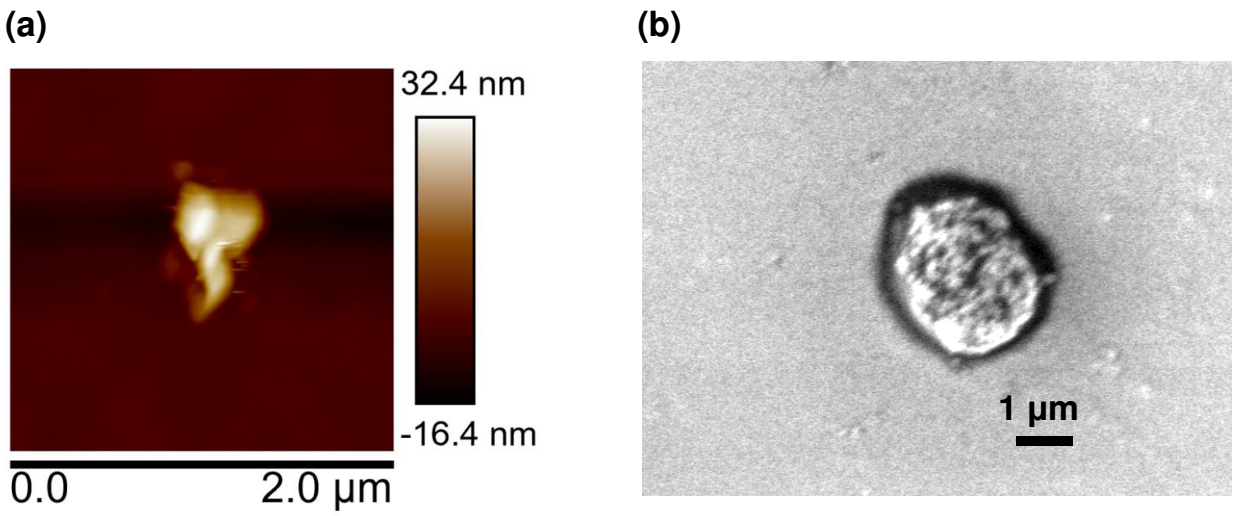

Figure S1. (a) The height profile of the BN flake measured by AFM in tapping mode. (b) The SEM image of a single BN flake.

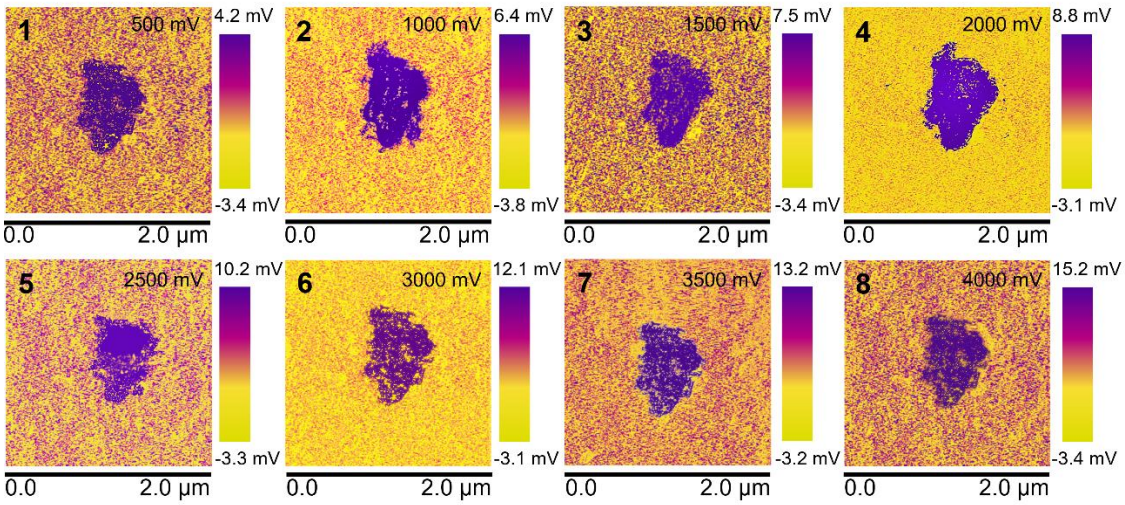

Figure S2. The piezoelectric response amplitude of a BN nanoparticle under different bias voltages ranging from 500 to 4000 mV.

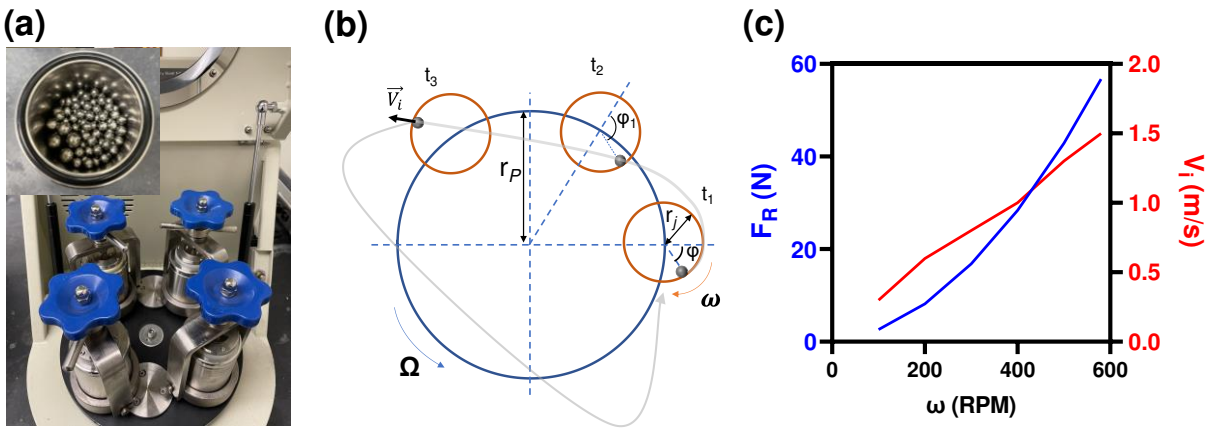

Figure S3. (a) Pictures of a jar filled with stainless steel balls and a planetary ball mill. (b) Schematic diagram showing the moving track of a single ball in the ball mill. (c) Radian impact force (F_R) and impact velocity (V_i) as functions of the jar rotation speed (ω).

Fig. S3b shows the moving track of a single ball during the BM process developed by a previous study.[1] The ball first moves along the wall from point t_1 (angular position of $\phi = 0$) to point t_2 (detachment point $\phi = \phi_1$). At point t_2, the centrifugal forces derived from disc rotation offset that from jar rotation. As a result, the ball detaches the wall and hits another side of the jar wall at an impact velocity (V_i).

The cosine of angular detachment position (cos Φ_1) can be calculated by

$$cos\phi_1 = -\frac{r_J(\Omega - \omega)^2}{r_P\Omega^2}$$

where r_J (2.6 cm) and r_P (90 cm) are the radius of the jar and planetary disk, respectively. ω and Ω (= ω/2) are the rotational speeds of the jar and disk, respectively.

Further, V_i can be obtained via

$$V_i^2 = \Omega r_P^2 + (\Omega - \omega)^2 r_J^2 + 2\Omega(\Omega - \omega) r_J r_P cos\phi_1$$

Assuming the ball travels a distance that equals to the r_J, the impact force F_R exerted on the wall could be calculated by the principle of kinetic energy conservation.

$$F_R = \frac{1}{2} m_b V_i^2 / r_J$$

where m_b (1.4 g) is the average weight of stainless steel ball. The F_R and V_i at different ω are shown in **Figure S3c**. For example, at ω of 580 rpm, V_i and F_R are given as 1.5 m/s and 57 N, respectively.

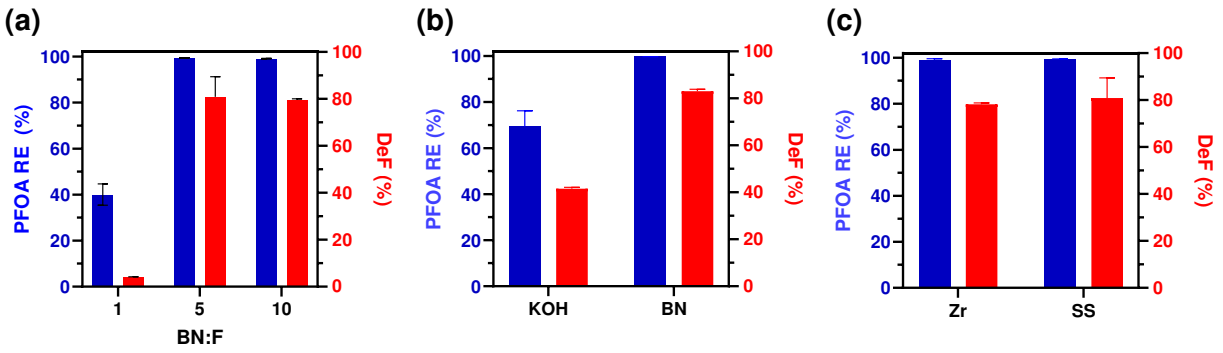

Figure S4. Effects of (a) the molar ratio of BN vs. [Fluorine on PFAS], (b) comilling reagents, and (c) ball materials on the PFOA removal efficiency and defluorination efficiency. For all the tests, the jar rotation speed was 580 rpm, and the treatment duration was one hour. In test set (b), 19 mmol of BN or KOH was co-milled with 0.23 mmol of PFOA. In test set (c), the performances of BN−BM treatment of PFOA were compared using Zr and SS balls at the same average weights.

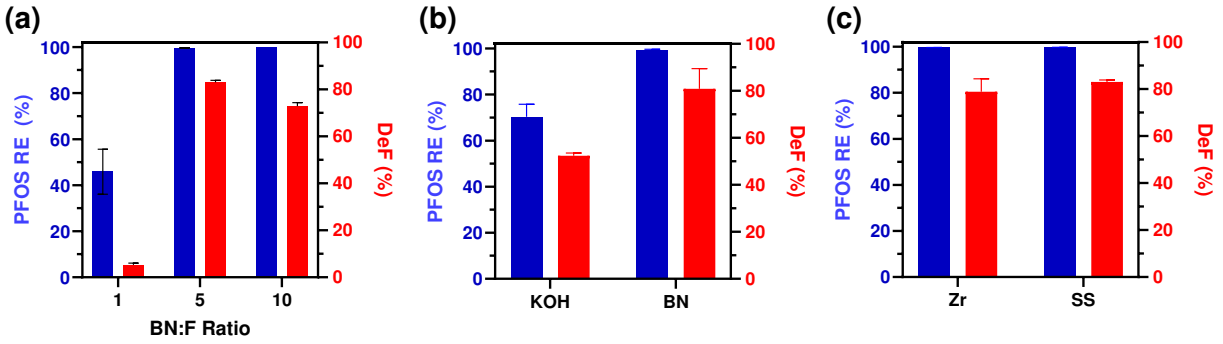

Figure S5. Effects of (a) the molar ratio of BN vs. [Fluorine on PFAS], (b) comilling reagents, and (c) ball materials on the PFOS removal efficiency and defluorination efficiency. For all the tests, the jar rotation speed was 580 rpm, and the treatment duration was one hour. In test set (b), 19 mmol of BN or KOH was co-milled with 0.23 mmol of PFOS. In test set (c), the performances of BN−BM treatment of PFOS were compared using Zr and SS balls at the same average weights.

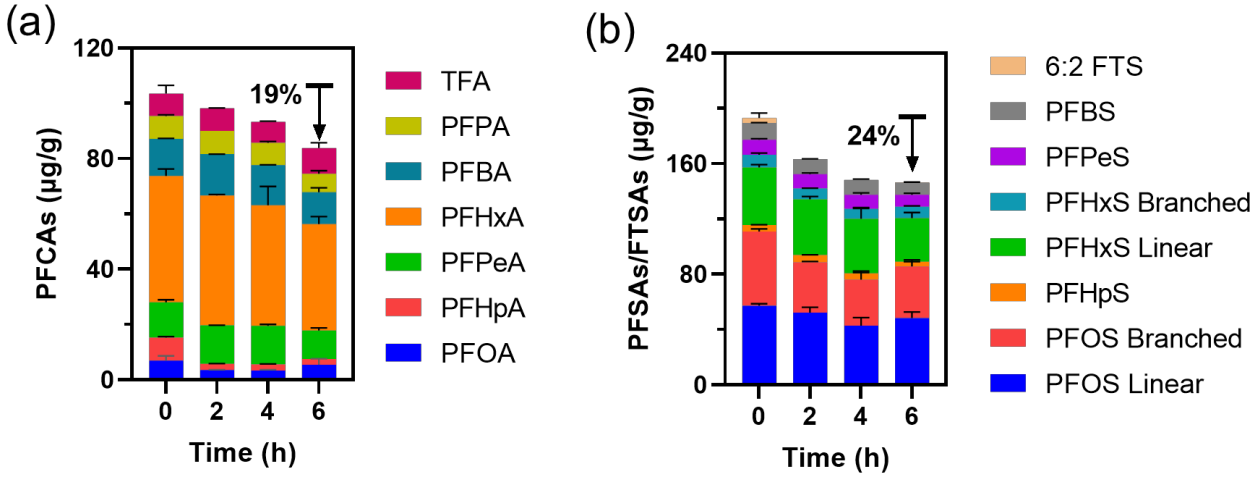

Figure S6. Destruction of (a) PFCAs and (b) PFSAs and FTS in sediment using KOH as the comilling reagent. Sediment (2 g) was amended with 20 mmol of KOH. The ball mill rotation speed was 580 rpm.

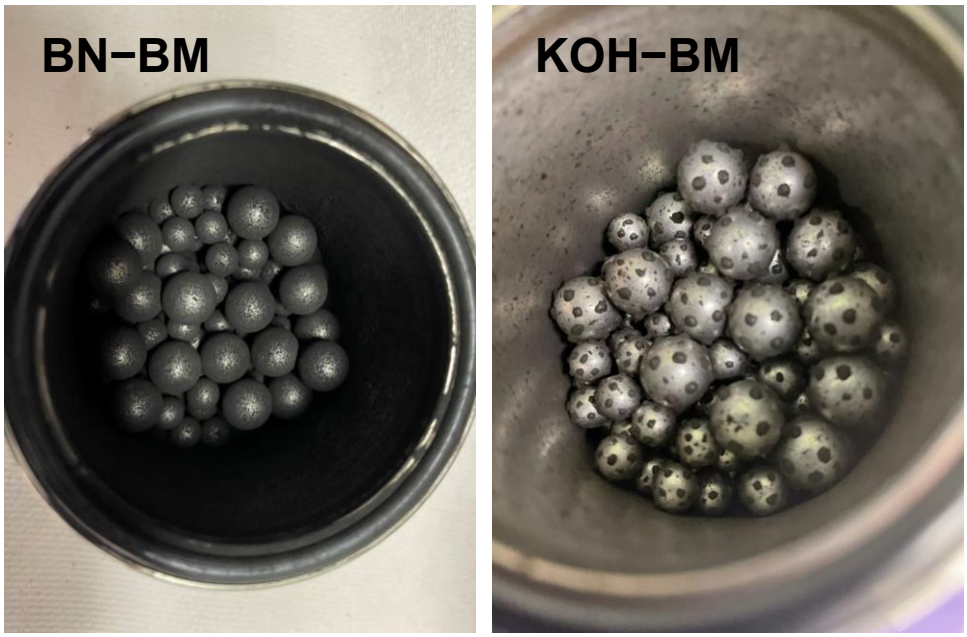

Figure S7. Photos of 20 mmol of BN co-milled with 2 g of sediment (left) and 20 mmol of KOH co-milled with 2 g of sediment (right) after 6 h of BM treatment.

The sediment contains 7.8% wt% of water. It is clearly shown that KOH powders agglomerate on the balls due to their hygroscopicity. The balls became sticky, and the free collision movement was largely retarded. This observation is in agreement with the previous report.[2] In contrast, the aggregation of BN was not observed because BN is not soluble in water and thus is not hygroscopic.

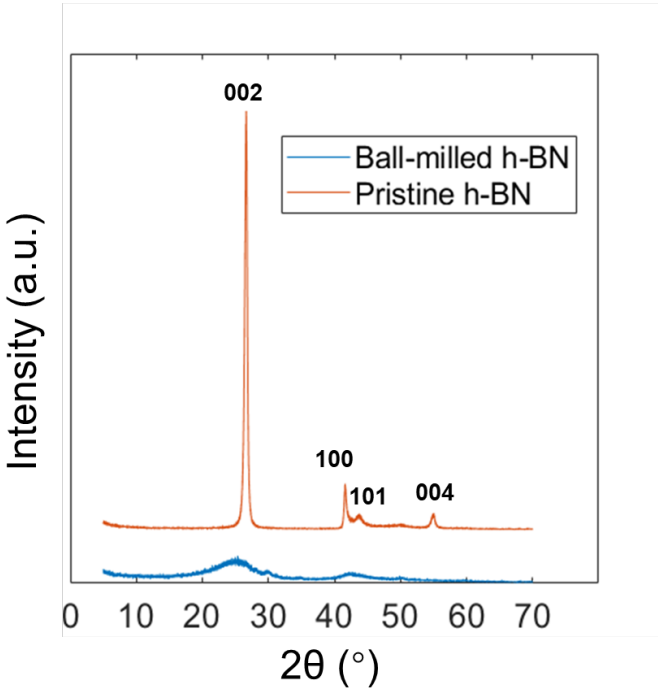

Figure S8. X-ray diffraction patterns of BN before and after 1 h of BM treatment.

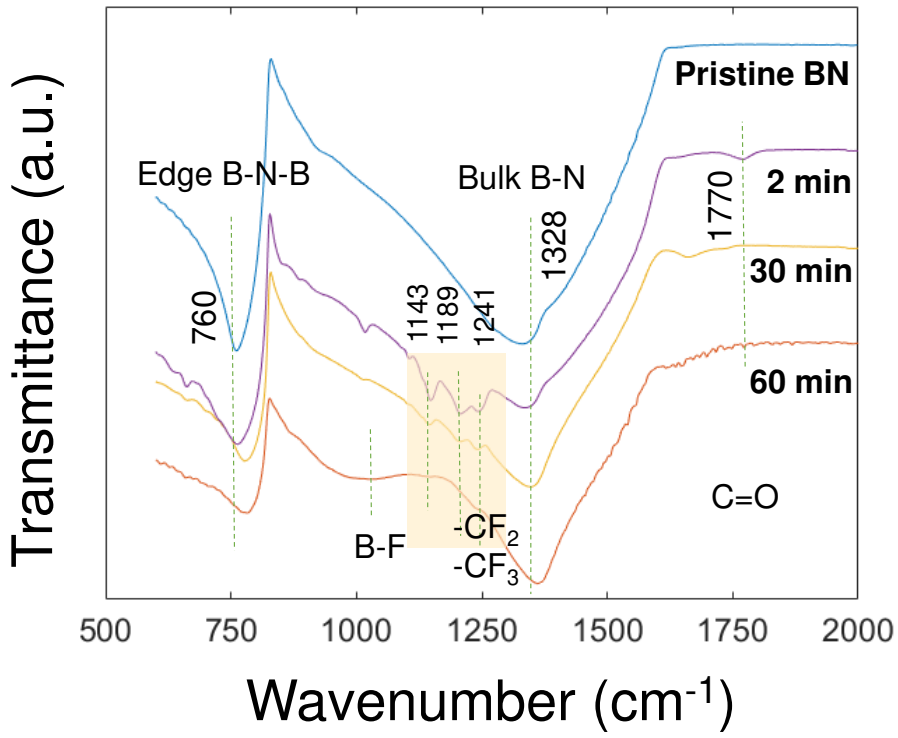

Figure S9. ATR-FTIR spectra of pristine BN and BN + PFOA mixture after 2, 30, and 60 min of BM treatment at jar speed of 580 rpm.

The spectrum of pristine BN exhibited lattice vibration modes derived from covalent bonds between nitrogen and boron atoms. BN was homogenized with PFOA by a two-minute quick ball milling. The homogenized sample shows the carboxylate group signal of PFOA at 1770 cm^{-1}, $-CF_2$, and $-CF_3$ groups from 1100 cm^{-1} to 1300 and C−F from 650 to 746 cm^{-1}. These PFOA features disappeared after 30 min ball milling.

FTIR also reveals the features of BN. The broad IR absorption peak at 1328 cm^{-1} can be assigned to the in-plane (bulk) B-N bond stretching vibration. The sharp peak between 750-800 cm^{-1} can be attributed to the out-of-plane (edge) B-N-B bending vibration.[3] With the increase of BM time, the peak representing bulk B-N bond remained intact while that related to edge B-N-B attenuated. These results suggest that BM impairs the edge B-N bonds of the BN flake.

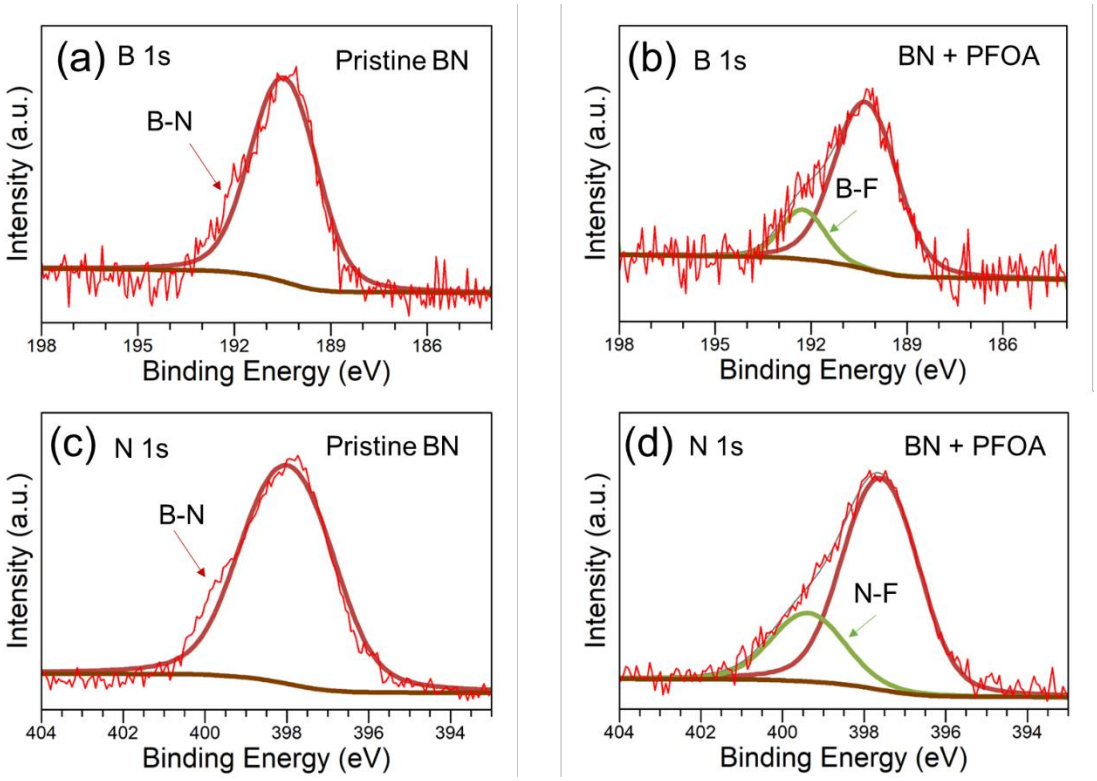

Figure S10. The B1s and N1s XPS spectra of (a, c) pristine BN and (b, d) BN + PFOA mixture after 1 h ball milling. After reacting with PFOA, both B1s and N1s peaks on BN were broadened. The shoulder peak at 192 eV matches the feature of the B-F bond, while that at 399 eV can be assigned to the N-F bond.[4]

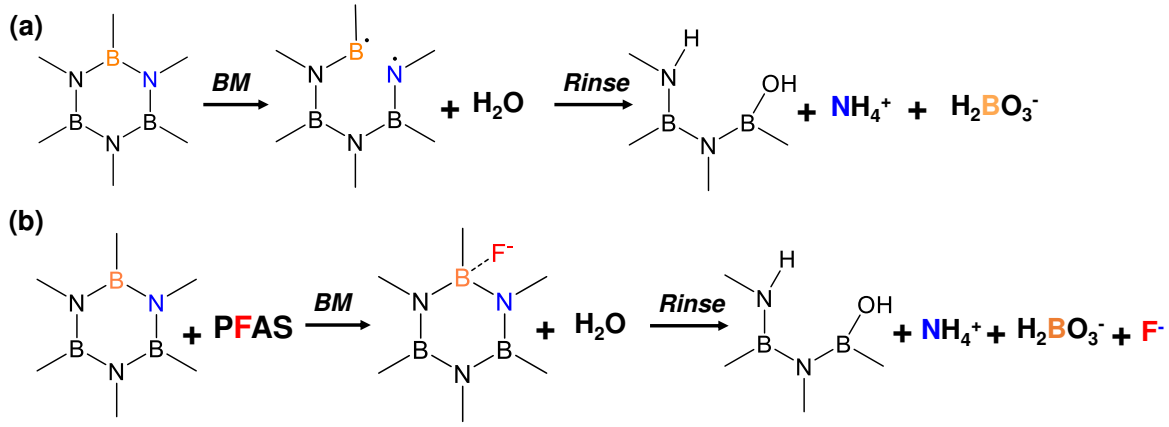

Figure S11. Schematic illustration of the B-N bond cleavage induced by BM and the dissolution by extraction (a) in the absence and (b) presence of PFAS. It is important to note that these are not balanced reactions. In the extract solution at pH 9.3 (**Table S3**), NH_3-N should be in a mix of NH_3 and NH_4^+ (pK_a = 9.26), and the boron compounds should be composed of H_3BO_3 and $H_2BO_3^-$ (pK_{a1} = 9.15).

References

(1) Chattopadhyay, P. P.; Manna, I.; Talapatra, S.; Pabi, S. K. A Mathematical Analysis of Milling Mechanics in a Planetary Ball Mill. *Mater. Chem. Phys.* **2001**, *68* (1), 85–94. https://doi.org/10.1016/S0254-0584(00)00289-3.

(2) Zhang, K.; Huang, J.; Yu, G.; Zhang, Q.; Deng, S.; Wang, B. Destruction of Perfluorooctane Sulfonate (PFOS) and Perfluorooctanoic Acid (PFOA) by Ball Milling. *Environ. Sci. Technol.* **2013**, *47* (12), 6471–6477. https://doi.org/10.1021/es400346n.

(3) Torii, S.; Jimura, K.; Hayashi, S.; Kikuchi, R.; Takagaki, A. Utilization of Hexagonal Boron Nitride as a Solid Acid–Base Bifunctional Catalyst. *J. Catal.* **2017**, *355*, 176–184. https://doi.org/10.1016/j.jcat.2017.09.013.

(4) Radhakrishnan, S.; Das, D.; Samanta, A.; de los Reyes, C. A.; Deng, L.; Alemany, L. B.; Weldeghiorghis, T. K.; Khabashesku, V. N.; Kochat, V.; Jin, Z.; Sudeep, P. M.; Martí, A. A.; Chu, C.-W.; Roy, A.; Tiwary, C. S.; Singh, A. K.; Ajayan, P. M. Fluorinated H-BN as a Magnetic Semiconductor. *Sci. Adv.* **2017**, *3* (7), e1700842. https://doi.org/10.1126/sciadv.1700842.